

Original Article



10.34172/EHEM.1498





Sustainable activated carbon prepared from beech wood residues for the adsorption of dyes: A Bayesian assessment of experimental data

Hosseinali Asgharnia^{1,2}, Mahdieh Haddadi³, Zeynab Gerinasab³, Mehdi Vosoughi^{4,5}, Fatemeh Aligholizadeh³, Hajar Tabarinia², Mohammad Shirmardi^{1,2}

¹Cellular and Molecular Biology Research Center, Health Research Institute, Babol University of Medical Sciences, Babol, Iran ²Department of Environmental Health Engineering, School of Public Health, Babol University of Medical Sciences, Babol, Iran ³Student Research Committee, Babol University of Medical Sciences, Babol, Iran

Abstract

Background: Removing dyes from wastewater is crucial for environmental protection and public health. Dyes used in various industries can be toxic and persistent, posing threats to aquatic ecosystems and human health.

Methods: This study examined the efficiency of beech wood-derived activated carbon (BW-AC) in removing Acid Red 18 (AR18) and Methylene Blue (MB) dyes. A batch adsorption procedure was used to investigate the impacts of various operational variables, including pH, contact time, adsorbent dosage, and initial dye concentration.

Results: Changes in pH did not significantly affect removal efficiency. However, increasing contact time and adsorbent dosage notably enhanced removal rates, achieving nearly complete removal after 180 minutes. Various statistical metrics were used to identify the best-fitting model, including the corrected Akaike information criterion (AIC_c) and Bayesian information criterion (BIC). The general order kinetic model provided the best fit to the experimental data based on its AIC_c values (range: -45.42 to 12.435) and BIC values (range: -48.16 to 6.67) for AR18. For MB dye, the ranges were -5.81 to 7.057 for AIC_c and -9.58 to 3.282 for BIC. Regarding the adsorption isotherms, the correlation capabilities of the models, as assessed by AIC_c and BIC, were ranked as follows for AR18: Freundlich, Liu, and Langmuir; while for MB dye, the ranking was Langmuir, Liu, and Freundlich.

Conclusion: The results demonstrate that BW-AC is a highly promising adsorbent for dye removal from aqueous solutions, offering a sustainable, environmentally friendly, and cost-effective solution for water and industrial wastewater treatment.

Keywords: Adsorption, Bayes theorem, Charcoal, Methylene Blue, Water

Citation: Asgharnia H, Haddadi M, Gerinasab Z, Vosoughi M, Aligholizadeh F, Tabarinia H, et al. Sustainable activated carbon prepared from beech wood residues for the adsorption of dyes: A Bayesian assessment of experimental data. Environmental Health Engineering and Management Journal. 2025;12: 1498. doi: 10.34172/EHEM.1498.

Article History: Received: 21 December 2024 Revised: 26 February 2025 Accepted: 11 March 2025

ePublished: 18 June 2025

*Correspondence to: Mohammad Shirmardi, Emails: m.shirmardi@ mubabol.ac.ir, shirmardim@ yahoo.com

Introduction

Environmental pollution is widely recognized as a significant global challenge. Among industrial pollutants, dyes are particularly harmful and extensively used in various industries, including textiles, food production, pharmaceuticals, cosmetics, paper manufacturing, leather processing, printing, and tanning (1,2). Approximately 700 000 tons of nearly 10 000 types of dyes and pigments are produced annually worldwide. These synthetic dyes can be classified based on their molecular structure, application, or solubility. For example, acid, basic, direct,

mordant, and reactive dyes are categorized as soluble dyes, whereas azo, disperse, sulfur, and vat dyes are considered insoluble dyes. Among these, azo dyes are the most extensively produced, accounting for approximately 70% of global dye production and representing the most widely used dye type worldwide (3,4).

Dyes in industrial effluents pose serious environmental and health hazards. They reduce sunlight penetration, impair visibility, and trigger eutrophication, disrupting photosynthesis in aquatic ecosystems and leading to ecological imbalances. Additionally, many dyes and

© 2025 The Author(s). Published by Kerman University of Medical Sciences. This is an open-access article distributed under the terms of the Creative Commons Attribution License (http://creativecommons.org/licenses/by/4.0), which permits unrestricted use, distribution, and reproduction in any medium, provided the original work is properly cited.

⁴Social Determinants of Health Research Center, Ardabil University of Medical Sciences, Ardabil, Iran

⁵Department of Environmental Health Engineering, School of Health, Ardabil University of Medical Sciences, Ardabil, Iran

their degradation products are toxic, carcinogenic, and mutagenic, contaminating water sources and potentially causing allergic reactions, dermatitis, and skin irritation in humans (5-8).

Among the various synthetic dyes, Acid Red 18 (AR18) and Methylene Blue (MB) are widely used in industrial applications. AR18, an azo dye containing sulfonic groups (-SO₃H) and azo (-N=N-) bonds, is largely employed in textile dyeing (wool, silk, and polyamide fibers) due to its solubility, stability, and affordability (9,10). It is also used in leather, paper, plastics, wood, pharmaceuticals, cosmetics, and food products. MB, a cationic dye, appears as a greenish-blue crystalline solid and is known for its applications in textiles, plastics, leather, and medicine (as a staining agent and therapeutic compound) (11-13). Despite their industrial importance, both dyes and their intermediate degradation products exhibit high toxicity, carcinogenicity, and mutagenicity, threatening aquatic life and human health (14,15).

Given these risks, effective wastewater treatment is crucial. Several physical, chemical, and biological methods have been explored for dye removal, including adsorption, chemical oxidation, membrane filtration, electrocoagulation, and biological treatments (16). Among them, adsorption has gained prominence due to its simplicity, cost-effectiveness, reusability, and high efficiency in removing persistent dye compounds. While other techniques—such as reverse osmosis (RO), nanofiltration (NF), and microfiltration (MF)-achieve high dye removal rates (~90%), they suffer from pore blockage, membrane fouling, and operational challenges. Similarly, advanced oxidation processes (AOPs), including photocatalysis and Fenton oxidation, generate reactive radicals for dye degradation but often require highenergy consumption and potentially toxic by-products. Biological methods such as activated sludge processes (ASPs), membrane bioreactor (MBR), sequencing batch reactor (SBR), and moving bed biofilm reactor (MBBR) have shown effective removal efficiencies. However, they often require large operational spaces, prolonged retention times, and face challenges in degrading recalcitrant dye components (17-21).

A comprehensive review by Dutta (21), analyzing dye removal methods from 1948 to 2020, revealed that adsorption is the most widely used method, accounting for 57.7% of reported cases, followed by photocatalysis (15.7%), Fenton processes (7.7%), coagulation and flocculation (5.4%), nanofiltration (3.2%), and ozonation (3%). The remaining percentage was attributed to other less commonly utilized techniques. These findings highlight adsorption as the predominant and preferred method for treating dye-contaminated wastewater.

Various adsorbents have been evaluated for dye removal, including activated carbon, bagasse ash, rice husk ash, cashew nut shell, plum kernel, rambutan peel, coconut

shell, magnesium chloride, and chitosan (11,22,23). Among them, activated carbon is widely regarded as the most effective due to its high porosity, large surface area, and exceptional adsorption properties. However, high production and regeneration costs often limit its large-scale applications (24-26). Additionally, many commercially available activated carbons are derived from non-renewable sources or require costly activation processes, making them economically unsustainable (27).

To address this challenge, the present study investigated the use of beech wood residues—a locally available, low-cost biomass—to produce activated carbon (BW-AC). This approach not only reduces production costs but also repurposes an abundant forestry byproduct into a sustainable and efficient adsorbent for dye removal. Unlike conventional activated carbons, BW-AC is a sustainable, eco-friendly, and practical alternative for dye removal. Furthermore, the integration of Bayesian statistical methods for model selection ensures a rigorous evaluation of adsorption kinetics and isotherms. Thus, this study provides a scientifically robust, economically feasible, and environmentally sustainable solution for wastewater treatment.

Materials and Methods Reagents and solutions

In this study, Acid Red 18 (AR18), also known as Ponceau 4R, Cochineal Red A, or New Coccine, was purchased from Alvan Sabet Company (Hamedan, Iran). Methylene Blue (MB), commonly referred to as basic blue 9 and alternatively known as methylthionine chloride, Aizen methylene blue, and Chromosmon, was obtained from Sigma Aldrich. Both dyes were used without additional purification due to their high laboratory-grade purity (≥88%). The key physicochemical properties of AR18 and MB are summarized in Table 1.

Preparation of beech wood activated carbon (BW-AC)

Beech wood waste was collected from beech-rich regions of Ardabil province, Iran. The wood was thoroughly washed with distilled water to remove impurities, and then dried in an oven at 110°C for 2 hours. After drying, it was ground and sieved to obtain uniform particle sizes. The sieved wood particles were soaked in 85% phosphoric acid at room temperature for 24 hours to initiate chemical activation. The acid-treated wood was then separated via filtration and washed repeatedly with distilled water to remove residual acid.

For the production of activated carbon, a pre-designed, sealed steel reactor equipped with unidirectional nozzles was used to facilitate nitrogen gas introduction and the expulsion of volatile gases generated during high-temperature processing. Before the experiment, the reactor was thoroughly cleaned, and the acid-treated wood was carefully loaded, ensuring all seals were securely

Table 1. Characteristics of the dyes used in this study (10,28,29)

Dye name	Molecular weight (g mol-1)	Chemical formula	Charge property	Water solubility	Chemical structure
Acid Red 18	604.48	$C_{20}H_{11}N_2Na_3O_{10}S_3$	Anionic	Soluble (40 g L ⁻¹)	NaO ₃ S N OH
Methylene Blue	319.85	C ₁₆ H ₁₈ N ₃ SCI	Cationic	Soluble (50 g L ⁻¹)	H ₃ C N S + CH ₃

closed. To establish an oxygen-free environment, nitrogen gas was introduced through one nozzle, while excess gas was vented through the opposing nozzle. The reactor was then placed in a furnace and heated to 650 °C for 2 hours to conduct pyrolysis under controlled conditions.

Following thermal activation, the carbonized material was cooled and washed repeatedly with distilled water until the rinse water reached a neutral pH. The resulting activated carbon was dried at 105 °C for 24 hours and sieved to obtain 595-841 μm particles. The prepared BW-AC was stored in an airtight container for subsequent use (18). The BET analysis showed that BW-AC had a specific surface area of 453 $m^2 \ g^{-1}$.

Adsorption experiments

A batch adsorption procedure using PET laboratory bottles containing 50-100 mL of dye solution was employed to investigate the adsorption of AR18 and MB. Initially, a 1000 mg L⁻¹ stock solution was prepared by dissolving precise amounts of AR18 and MB in distilled water, which was then diluted to obtain working solutions of desired concentrations. The following key operational parameters were systematically evaluated.

Effect of pH

The influence of pH on AR18 and MB adsorption was investigated over a pH range of 3, 5, 7, 9, 11, and the natural pH of the solution. Experiments were conducted using an adsorbent dosage of 1 g L⁻¹, a contact time of 2 h, and an initial dye concentration of 100 mg L⁻¹ at room temperature. The pH of the solutions was adjusted using 0.1 M HCl or 0.1 M NaOH before adding the adsorbent.

Effect of contact time

To explore the impact of contact time on the adsorption of AR18 and MB dyes, it was varied from 5 to 180 minutes. These experiments were carried out under the natural pH conditions of the dye solutions, with an adsorbent dosage of 1 g $\rm L^{-1}$, and initial dye concentrations of 50 and 100 mg $\rm L^{-1}$. All other experimental parameters remained constant.

Effect of adsorbent dosage

The role of adsorbent dosage in AR18 and MB adsorption

was assessed by testing various dosages (0.5, 0.75, 1, 1.25, 1.5, 1.75, 2, and 2.5 g L⁻¹). Experiments were performed at room temperature, natural pH, an initial dye concentration of 100 mg L⁻¹, and a contact time of 3 hours, while keeping all other conditions unchanged.

Effect of initial dye concentration

To examine the effect of initial dye concentration, it was varied from 5 to 250 mg L⁻¹. These experiments were conducted at room temperature, under natural pH conditions, with an adsorbent dosage of 1.5 g L⁻¹ and a contact time of 3 hours.

Throughout the adsorption tests, the solutions were continuously agitated using a magnetic stirrer or an incubator shaker at 250 rpm to ensure uniform mixing. Parallel blank experiments (without BW-AC) were performed under identical conditions to account for potential dye adsorption onto the reaction vessels and to assess the influence of other factors. All adsorption experiments were conducted in triplicate, and mean values were reported for reliability.

Unary and binary adsorption of dyes from real water samples

This study also investigated AR18 and MB adsorption from real water samples to evaluate the influence of naturally occurring ions and organic/inorganic compounds. The adsorption experiments were conducted using seawater, well water, and tap water, with distilled water serving as the control to establish a baseline for adsorption performance. The adsorbent dosage was 1.5 g $\rm L^{-1}$, and the initial dye concentration was maintained at 100 mg $\rm L^{-1}$. To simulate real-world conditions, the natural pH of each water sample was maintained. Adsorption studies were performed both individually (unary system) for each dye and simultaneously (binary system) to evaluate potential competitive adsorption effects. All other experimental conditions remained unchanged.

Adsorption kinetics

Adsorption kinetics experiments are essential for understanding the speed, pathways, and primary

mechanisms involved in dye adsorption. They play a crucial role in determining the factors that influence reaction rates and the mechanisms controlling the adsorption process, such as chemical reactions or diffusion mechanisms (30). Data obtained from studying the effect of contact time were utilized to investigate the adsorption kinetics.

The kinetic behaviors of the adsorption process were analyzed using the nonlinear equations for the pseudo-first order (PFO), pseudo-second-order (PSO), general-order (GOK), and intraparticle diffusion models, as represented by Equations 1-4, respectively (31-35):

$$q_t = q_e \cdot [1 - \exp(-k_f \cdot t)]$$
 (1)

$$q_{t} = \frac{k_{s} \times q_{e}^{2} \times t}{1 + a \times k \times t} \tag{2}$$

$$q_{t} = q_{e} \left\{ 1 - \left[\frac{1}{[1 + (n-1) \times k_{N} \times (q_{e})^{(n-1)} \times t}] \right]^{\frac{1}{n-1}}$$
 (3)

$$q_t = k_{id}\sqrt{t} + C \tag{4}$$

In these equations, t, q_t , and q_e represent the contact time (min), the quantity of dye molecules adsorbed at a particular time t (mg g⁻¹), and the quantity of dye molecules adsorbed upon reaching equilibrium (mg g⁻¹), respectively. The symbols k_p , k_s , and k_N denote the pseudofirst-order rate constant (min-1), the pseudo-second order rate constant (g mg⁻¹ min⁻¹), and the general order rate constant (min⁻¹ (g mg⁻¹)n⁻¹), respectively; n represents the order of kinetic adsorption, which may be an integral or fractional number. Moreover, the parameters k_{cl} (mg g⁻¹ h^{-0.5}) and C (mg g⁻¹) are key components of the intraparticle diffusion model for adsorption. The k, parameter represents the adsorption rate constant, reflecting the rate at which AR18 or MB diffuses into the pores of the BW-AC particles. The parameter C relates to the boundary layer thickness that affects the adsorption process. The values of k_{id} and C can be directly obtained from the slope and intercept of the plot q, versus t^{0.5}, respectively.

Adsorption isotherm experiments

The study of adsorption isotherms is crucial for gaining insights into the mechanisms of the adsorption process and determining the maximum adsorption capacity (36). The experimental data derived from analyzing the influence of initial dye concentration were employed to evaluate the adsorption isotherms. The experiments were conducted under optimal conditions determined in earlier tests. The experimental data were fitted to the nonlinear equations for the Langmuir (37), Freundlich (38), and Liu (39) isotherm models (Equations 5-7).

$$q_e = \frac{Q_{\text{max}} \times K_L \times C_e}{1 + K_L \times C_e} \tag{5}$$

$$q_{e} = K_{F} \times C_{e}^{1/n_{F}} \tag{6}$$

$$q_{e} = \frac{Q_{\text{max}} \times (K_{g} \times C_{e})^{n_{L}}}{1 + (K_{g} \times C_{e})^{n_{L}}}$$
(7)

In these equations, q_e , C_e , and Q_{max} represent the quantity of dye adsorbed at the equilibrium time (mg g⁻¹), the equilibrium concentration of dye (mg L⁻¹), and the maximum adsorption capacity of the adsorbent (mg g⁻¹), respectively. K_L , K_F , and K_g stand for the Langmuir equilibrium constant (L mg⁻¹), the Freundlich equilibrium constant [mg g⁻¹ × (mg L⁻¹) -1/nF], and the Liu equilibrium constant (L mg⁻¹), respectively. Moreover, n_F and n_L indicate the dimensionless exponents linked to the Freundlich and Liu models, respectively.

Determination of final dye concentration

A UV-Vis spectrophotometer (model DR5000, Hach Company, USA) was used to measure dye concentrations. Calibration curves were established using standard solutions to correlate absorbance values with dye concentrations. The absorbance of each standard solution was measured at 509 nm for AR18 and 665 nm for MB (40,41).

Following each experimental run, samples were filtered using 0.22- μ m membrane filters to remove adsorbent particles before analysis. Removal efficiency and adsorption capacities at time t (q_t, mg g⁻¹) and equilibrium (q_e, mg g⁻¹) were respectively calculated using the following equations:

$$Dy\ removal(\%) = \frac{\left(C_o - C_e\right)}{C_o} \times 100 \tag{8}$$

$$q_{t} = \frac{\left(C_{o} - C_{t}\right) \times V}{M} \tag{9}$$

$$q_e = \frac{(C_o - C_e) \times V}{M} \tag{10}$$

In this context, C_0 and C_e (mg L⁻¹) represent the initial and equilibrium concentrations of AR18 and MB dyes in the solution. The variable M (g) is the BW-AC adsorbent dosage, while V (L) indicates the volume of the solution. Additionally, C_t (mg L⁻¹) refers to the concentration of AR18 and MB dyes at time t, and q_t (mg g⁻¹) represents the adsorption capacity of AR18 and MB dyes at time t.

Model selection criteria

A nonlinear approach was adopted to analyze kinetics and isotherms data using the Levenberg-Marquardt algorithm and the Simplex method in OriginPro 2018 software. The coefficient of determination (R²) has been widely used

for comparing and selecting the best-fitted model in adsorption kinetics and isotherm studies. However, R² has notable limitations, particularly its failure to account for the number of parameters in a model, which often leads to a preference for more complex models with a higher number of parameters. As a result, it is regarded as an inadequate criterion for model selection (42).

A more robust approach for evaluating model goodness-of-fit, which incorporates the number of parameters, is the information criteria (ICs). The use of ICs for model selection is beneficial due to their straightforward interpretation and applicability to both nested and non-nested models. When comparing models fitted to the same dataset, the model with the lowest or most negative value is typically identified as the best fit (42). Even at low noise levels in the data, R2 and the chisquare test, which are also recognized as criteria for model selection, correctly identified the appropriate model only 28%-43% of the time, exhibiting a strong preference for highly parameterized models. In contrast, informationbased criteria such as the Akaike information criterion (AIC) and Bayesian information criteria (BIC) correctly selected the appropriate model 80% of the time under the same conditions, despite a slight bias towards models with fewer parameters (43,44). Therefore, AIC and BIC are recommended as the preferred criteria for comparing nonlinear models (44).

The AIC, introduced by Hirotugu Akaike (45), serves as a comparative indicator of model fit, assessing the quality of fit provided by a statistical model. This criterion is grounded in the concept of information theory and quantifies the relative information loss incurred when a specific model is employed to represent a realworld phenomenon. Akaike established a connection between predictions derived from the Kullback-Leibler information measure and the maximized support function, facilitating a more integrated approach to model selection and analysis of complex datasets. However, the effectiveness of AIC may diminish when the number of parameters significantly exceeds the sample size, as noted by Sugiura (46) and Sakamoto et al (47). To address this issue, Sugiura (46) introduced a second-order modification of the AIC, known as the corrected Akaike information criterion (AIC). Burnham and Anderson (48) recommend using the AIC, when the ratio of sample size to the number of parameters (n/p) is small (e.g., when n/p < 40). When this ratio is sufficiently large, both AIC and AIC are expected to yield similar results (49).

The BIC is another statistical approach grounded in information theory, distinguished by its more stringent penalty on the number of parameters included in the model compared to AIC (50,51). BIC is a widely used metric for model selection. When comparing two models using BIC, the difference in BIC values (Δ BIC) can provide valuable insights into their relative fit. According

to the established guidelines, if the difference between the BIC values of two models (Δ BIC) is less than 2, the models are generally interpreted as not differing significantly in their fit to the data. This suggests that the models can be regarded as equally well fitted. Conversely, when Δ BIC \geq 10, the model with the lowest BIC value is considered to be definitively the best-fitted model, indicating very strong evidence in favor of that model. In cases where $2 < \Delta$ BIC < 6, the model with the lower BIC value is regarded as a potential best-fitted model. When $6 < \Delta$ BIC < 10, there is a strong likelihood that the model with the lower BIC value is indeed the best-fitted model (52-54).

Alongside traditional statistical criteria, including standard deviation (SD), coefficient of determination (R^2), and adjusted coefficient of determination (R^2 _{adj}), the AIC and BIC were used, as detailed in the existing literature (54-57), to select and rank the optimal models for the kinetics and isotherm data analyzed in this research. The mathematical expressions for R^2 , R^2 _{adj}, SD, AIC, and BIC are provided in the following equations (Eqs. 11-15). The results related to these model selection criteria are detailed in the Results and Discussion sections.

$$R^{2} = \left(\frac{\sum_{i}^{n} (q_{i,\exp} - \overline{q}_{\exp})^{2} - \sum_{i}^{n} (q_{i,\exp} - q_{i,\text{mod}el})^{2}}{\sum_{i}^{n} (q_{i,\exp} - \overline{q}_{\exp})^{2}}\right)$$
(11)

$$R^{2}_{adj} = 1 - \left(1 - R^{2}\right) \times \left(\frac{n - 1}{n - p - 1}\right)$$
 (12)

$$SD = \sqrt{\left(\frac{1}{n-p}\right) \times \sum_{i}^{n} \left(q_{i,\exp} - q_{i,\text{mod }el}\right)^{2}}$$
 (13)

$$AIC = nLn\left(\frac{RSS}{n}\right) + 2(p+1) \to \qquad \text{when } \frac{n}{p} \ge 40$$

$$AIC_c = nLn\left(\frac{RSS}{n}\right) + 2(p+1) + \frac{2(p+1)(p+2)}{n-p-2} \to \text{when } \frac{n}{p} < 40$$
(14)

$$BIC = nLn\left(\frac{RSS}{n}\right) + (p+1)Ln(n) \tag{15}$$

In the above-mentioned equations, $q_{i,exp}$ represents the individual experimental q value, while $q_{i,model}$ is the individual theoretical q value predicted by the model. \overline{q}_{exp} is the average of all experimental q values measured; n indicates the total number of experiments conducted; p refers to the number of parameters in the fitted model; and RSS stands for residual sum of squares (53,55).

Results

Effect of pH on dye adsorption

This study investigated the effect of solution pH on the removal efficiency of AR18 and MB using BW-AC adsorbent under varying pH conditions. The results, shown in Figure 1 (A and B), indicate that the removal

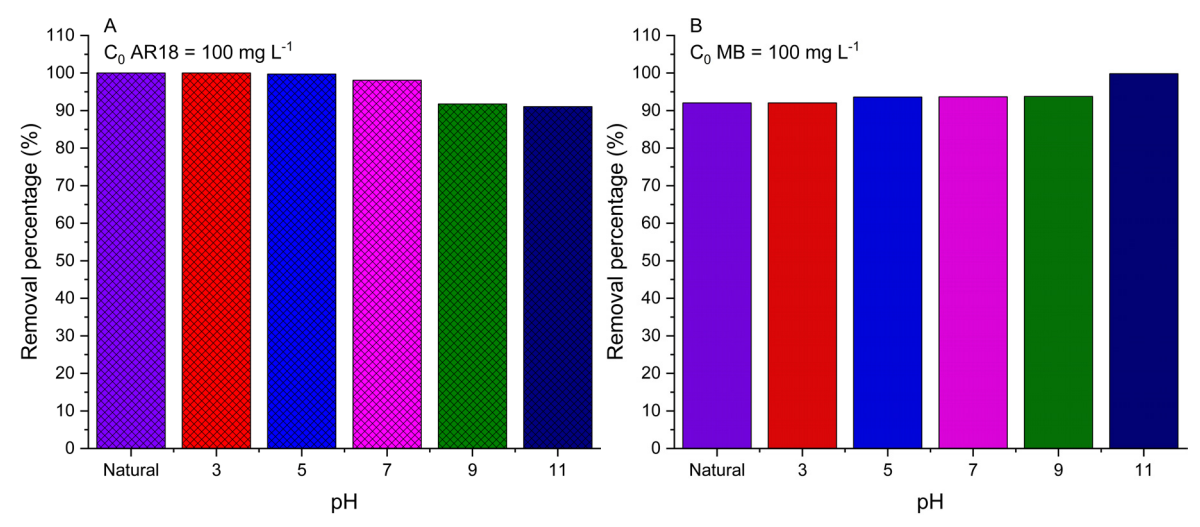


Figure 1. Effect of pH on the adsorption of AR18 and MB dyes onto BW-AC adsorbent. Experimental conditions: initial dye concentration = 100 mg L⁻¹, room temperature, adsorbent dosage = 1 g L⁻¹, and contact time = 2 h

efficiency of both dyes at an initial concentration of 100 mg L⁻¹ was minimally influenced by changes in pH. For AR18, the highest removal efficiency (>99.9%) was observed in the acidic pH range of 3-5, while the lowest removal efficiency (91%) occurred at pH 11. In contrast, the removal efficiency of MB dye increased from 92% at pH 3 to 99.9% at pH 11. Given the negligible variations in dye removal efficiency across the examined pH range and considering that natural pH conditions more accurately reflect real-world scenarios, the natural pH of the solution was selected as the optimal pH for subsequent experiments.

Effect of contact time and kinetic studies

The kinetics of AR18 and MB dye removal were evaluated using various kinetic models, as illustrated in Figure 2 (A-H), and their parameters are summarized in Table 2. BW-AC demonstrated rapid adsorption rates for both dyes. At an initial concentration of 50 mg L⁻¹, the removal efficiency reached 98.6% for AR18 and 91.53% for MB within the first 5 minutes. However, at a higher initial concentration of 100 mg L⁻¹, the removal rates decreased to 65.11% for AR18 and 83.6% for MB under the same conditions. After 180 minutes, the total removal rates reached 100% for AR18 and 99.24% for MB at 50 mg L^{-1} , while at 100 mg L^{-1} , the removal efficiencies were 89% for AR18 and 94% for MB. The system approached equilibrium after 20 minutes for the 50 mg L-1 concentration and after 60 minutes for the 100 mg L⁻¹ concentration, regardless of the dye type. Among the kinetic models analyzed, the GOK model provided the best fit to the experimental data, as indicated by the lowest AIC and BIC values (Table 2).

Effect of adsorbent dosage

The effect of BW-AC dosage (0.5-2.5 g L⁻¹) on dye removal efficiency and adsorption capacity (q_e), is illustrated in Figure 3. Increasing the adsorbent dosage enhanced dye

removal efficiency up to 1.5 g L⁻¹, beyond which it plateaued. For AR18, the removal efficiency increased from 75% to 100%, while for MB, it increased from 71.5% to 99.7%.

Effect of initial dye concentration and adsorption isotherms

The dye removal efficiency decreased with increasing initial dye concentration, as shown in Figure 4 (A-D). For AR18, the removal efficiency decreased from 100% to 81.37%, while for MB, it decreased from 99.3% to 70% as the initial dye concentration increased from 5 to 250 mg L⁻¹. A more significant reduction in removal efficiency was observed at concentrations above 175 mg L⁻¹. On the other hand, the adsorption capacity (q_e) increased significantly with higher initial dye concentrations. For AR18, it increased from 3.33 to 136 mg g⁻¹, and for MB, it increased from 3.22 to 116.5 mg g⁻¹, as the initial concentration increased from 5 to $250 \, \text{mg L}^{-1}$. These results highlight the strong dependence of adsorption capacity on the initial dye concentration. Nonlinear isotherm analyses showed that the Freundlich model best described AR18 adsorption, while the Langmuir model was more accurate for MB adsorption. The isotherm parameters and statistical comparisons are detailed in Table 3.

Unary and binary adsorption of dyes from real water samples

The experimental design aimed to assess the impact of complex water matrices on the adsorption process and to compare the results with those obtained in distilled water, thereby providing insights into the practical applicability of the adsorbent in diverse aqueous environments. The experimental results revealed exceptional adsorption efficiency for both AR18 and MB across all tested water samples. In both unary and binary adsorption systems, the removal percentages consistently exceeded 99%, as shown in Figure 5.

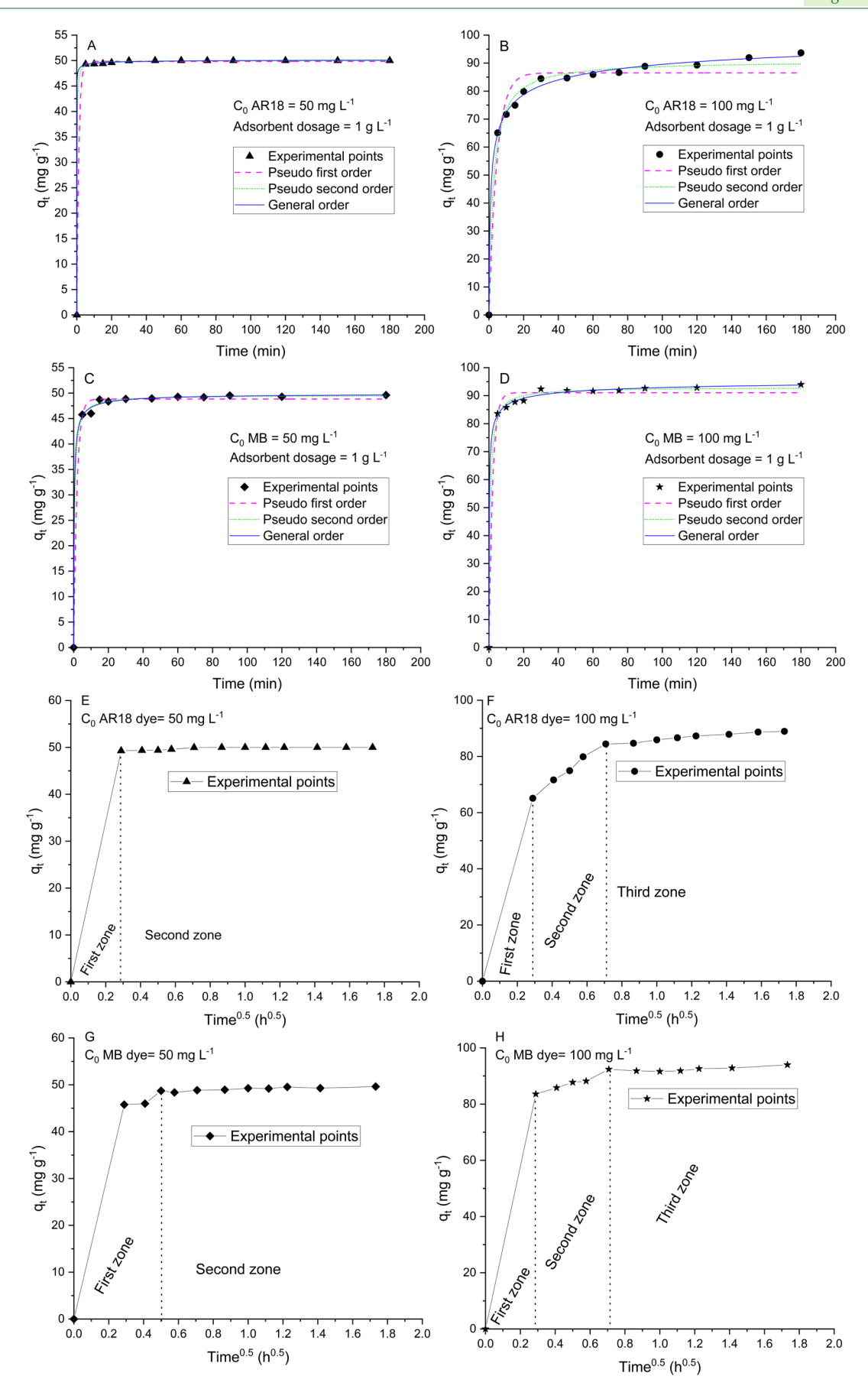


Figure 2. Kinetic models for the adsorption of AR18 (A and B) and MB (C and D), and intraparticle diffusion models for AR18 (E and F) and MB (G and H) at room temperature. Experimental conditions: adsorbent dosage = 1 g L^{-1} ; dye concentrations = $50 \text{ and } 100 \text{ mg L}^{-1}$, and natural pH of solution

Table 2. Parameters of the fitted models for the adsorption of AR18 and MB dyes (Experimental conditions: room temperature; adsorbent dosage=1 g L $^{-1}$; dye concentrations=50 and 100 mg L $^{-1}$, and natural pH of solution)

Kinotio navemetar	AR18		МВ	
Kinetic parameter	50 mg L-1	100 mg L ⁻¹	50 mg L ⁻¹	100 mg L ⁻¹
Pseudo-first order				
q _e (mg g ⁻¹)	49.85	85.21	48.84	91.058
k _f (min ⁻¹)	0.895	0.236	0.53	0.477
R^2_{adj}	0.9997	0.97	0.995	0.992
SD (mg g ⁻¹)	0.25	4.153	0.93	2.39
RSS	0.68951	189.74	8.76	56.94
AIC _c	-29.52	43.52	5.23	27.68
BIC	-30.48	42.55	3.68	26.14
t _{1/2} (min)	0.775	2.94	1.31	1.452
t _{0.95} (min)	3.35	12.7	5.65	6.28
Pseudo-second orde	er			
q _e (mg g ⁻¹)	50.005	89.12	49.58	93
K _s (min ⁻¹)	0.214	0.0053	0.0425	0.0162
R^2_{adj}	0.99989	0.996	0.998	0.998
SD (mg g ⁻¹)	0.147	1.46	0.509	1.158
RSS	0.23808	23.43	2.588	13.41
AIC _c	-43.34	16.325	-9.41	10.33
BIC	-44.31	15.353	-10.95	8.79
t _{1/2} (min)	0.094	2.136	0.475	0.662
t _{0.95} (min)	1.77	40.59	9.016	12.574
General order				
q _e (mg g ⁻¹)	50.405	93.39	50.02	97.16
K _N (min ⁻¹)	0.043	2.63×10 ⁻⁴	0.0153	1.019×10 ⁻⁴
N	3.69	4.516	2.44	3.52
R^2_{adj}	0.9999	0.998	0.999	0.999
SD (mg g ⁻¹)	0.12	1.115	0.5	0.875
RSS	0.14537	12.45	2.359	6.89
AIC _c	-45.42	12.435	-5.81	7.057
BIC	-48.16	6.67	-9.58	3.282
t _{1/2} (min)	0.00123	1.77	0.28	0.18
t _{0.95} (min)	0.72	143.32	12	72.323

Discussion

Effect of pH on dye adsorption

The pH of a solution plays a critical role in dye adsorption by influencing electrostatic interactions between the adsorbent and the adsorbate. Variations in pH can significantly alter the surface characteristics of the adsorbent, impacting its acidic or basic nature and, consequently, its adsorption capacity (58). For AR18, an anionic dye, adsorption onto BW-AC is primarily driven by electrostatic interactions. At lower pH levels, the protonation of functional groups on the surface of BW-AC enhances AR18 adsorption due to increased positive charges. In contrast, at alkaline pH, the presence of OHions and the negative charges on both the adsorbent

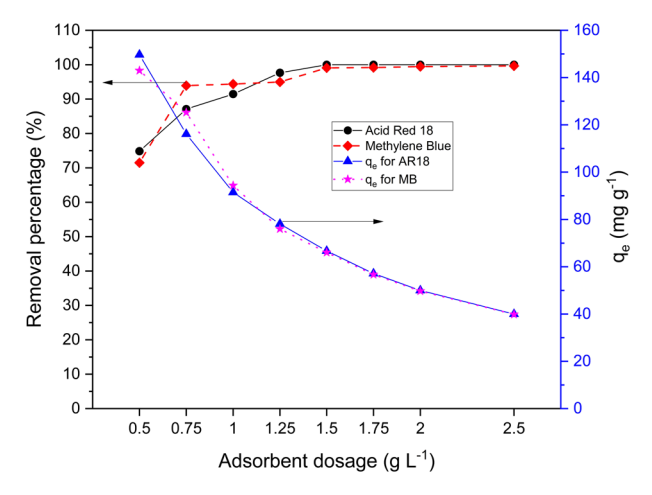


Figure 3. Effect of adsorbent dosage on the adsorption of AR18 and MB dyes. Experimental conditions: natural pH, room temperature, contact time = 180 min, and initial dye concentration = 100 mg L^{-1}

and AR18 molecules lead to repulsive forces, reducing adsorption efficiency. Although adsorption persisted under alkaline conditions, it was slightly diminished due to weaker electrostatic attraction. Additional mechanisms, such as van der Waals and dispersive forces, also contributed to the adsorption process (59).

Previous studies have demonstrated that the optimal pH for removing anionic direct dyes using activated carbon is pH 3 or lower. Namasivayam and Kavitha (60) confirmed the suitability of acidic pH for the adsorption of Congo Red, an anionic azo dye, on activated carbon derived from coir pith, an agricultural solid waste. Our findings suggest that the adsorption of AR18 onto BW-AC remains relatively constant across different pH values. This indicates that the adsorbent may possess high stability and reliable performance across a broad pH spectrum, potentially attributable to its structural or chemical composition. This insight is particularly relevant for industrial applications where pH fluctuations are common, necessitating the use of adsorbents that retain their effectiveness under varying pH conditions. In contrast, MB, a cationic dye, exhibits the opposite behavior. Its removal efficiency increases with pH, reaching 99.9% at pH 11. This is due to the higher presence of OH- ions at higher pH levels, which decreases the protonation of the BW-AC surface. As a result, the surface becomes more negatively charged, enhancing the electrostatic attraction to positively charged MB ions (61,62).

Effect of contact time and kinetic studies

The adsorption kinetics of AR18 and MB dyes at the adsorbent-solution interface were evaluated using kinetic models (Equations 1–4). The analyses aimed to elucidate the adsorption mechanisms, estimate removal rates, determine equilibrium times, identify rate-controlling diffusion steps, and assess the role of chemisorption in the adsorption process (42).

Figure 2 (A-H) shows that adsorption rates depend on

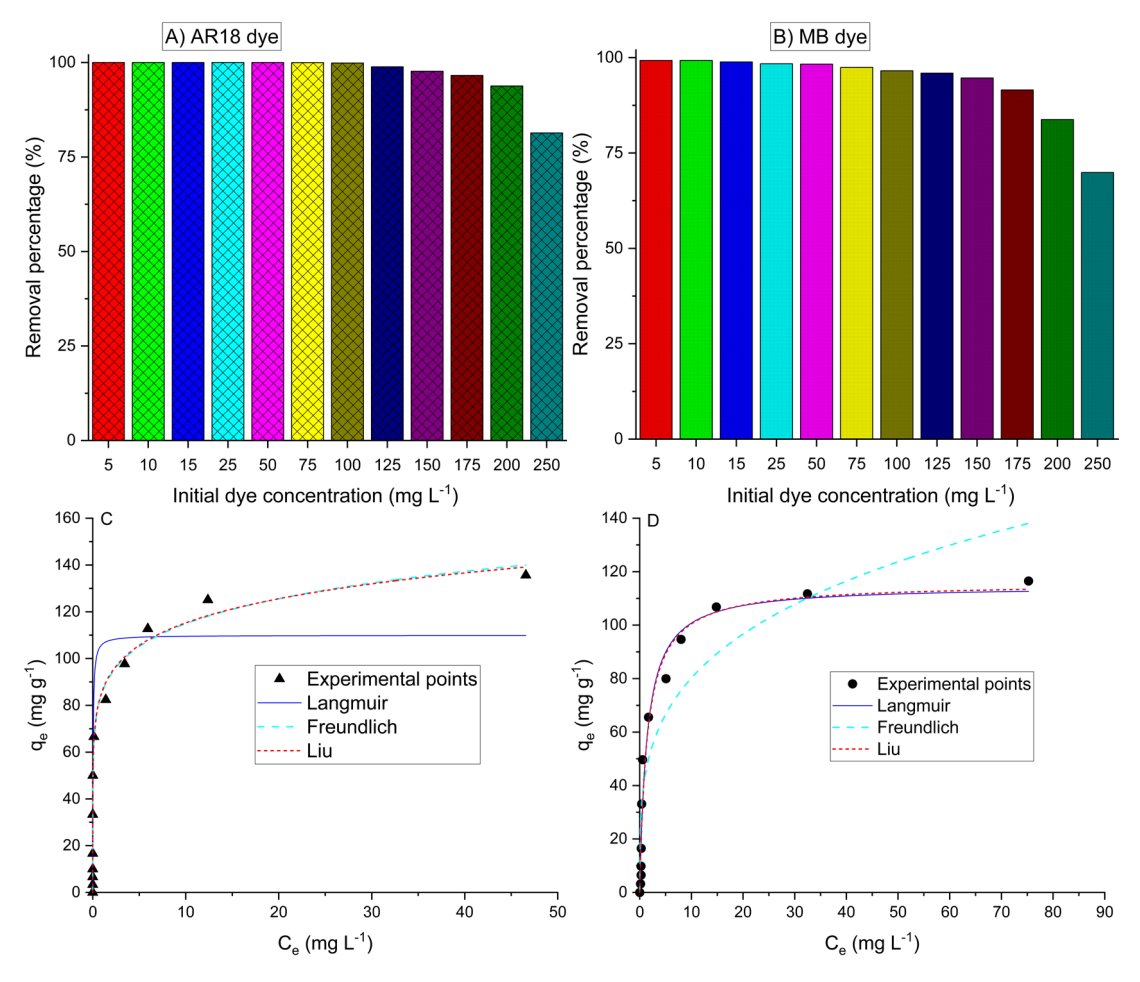


Figure 4. Adsorption of AR18 (A) and MB (B) as a function of initial dye concentration, with corresponding isotherm models for AR18 (C) and MB (D) using BW-AC adsorbent. Experimental conditions: room temperature; adsorbent dosage = 1.5 g L⁻¹; contact time = 180 min, and natural pH of the dye solution

dye concentration, with equilibrium being achieved faster at lower concentrations. The initial rapid adsorption is attributed to the abundance of available adsorption sites, which gradually become occupied, slowing the process over time. Nonlinear fitting of kinetic models revealed that the GOK model provided the best fit for both dyes, as indicated by the lowest AIC and BIC values, except for MB at 50 mg L⁻¹. For instance, at 50 mg L⁻¹AR18, the AIC values for the PFO, PSO, and GOK models were -29.52, -43.34, and -45.42, respectively, with corresponding BIC values of -30.48, -44.31, and -48.16, respectively. A comparison of PFO with PSO indicates that PSO is 1004 times more likely to be correct than PFO. Additionally, the lower BIC value of PSO further supports its accuracy, with a BIC difference greater than 10, establishing a strong preference for PSO over the PFO model.

In contrast, at 50 mg L^{-1} , a comparison of PSO with GOK indicates that GOK is 2.83 times more likely to be correct than PSO based on AIC_c values. The lower BIC value of GOK also suggests that it is the most accurate and best-fitted model. For MB at 50 mg L^{-1} , the comparison between PSO and GOK reveals that PSO is 6 times more likely to be correct based on the AIC_c value. However, as their Δ BIC is less than 2, this comparison remains

inconclusive. For more detailed comparisons and additional information on the evaluated kinetic models, please refer to Table 2. Statistical analyses such as SD, R^2_{adj} , AIC_c, and BIC confirm that the GOK model overall provides the best fit to the experimental data.

Table 2 also includes half-life $(t_{1/2})$ and time to 95% saturation (t_{0.95}) values, which represent the time required to achieve 50% and 95% of the maximum adsorption capacity, respectively. These parameters facilitate the comparison of kinetic models regardless of their rate constants and units. Given that the GOK was identified as the optimal kinetic model for this study, its $t_{1/2}$ for AR18 adsorption onto BW-AC ranged from 0.00123 to 1.77 min, while $t_{0.95}$ varied from 0.72 to 143.32 min. For MB, $t_{1/2}$ and $t_{0.95}$ ranged from 0.18 to 0.28 min and 12 to 72.32 min, respectively. These results suggest that higher adsorption capacities require longer equilibrium times. Given that the isotherm experiments were conducted at various initial concentrations up to 250 mg L⁻¹, a contact time of 180 minutes was used for adsorption equilibrium experiments to ensure that all examined dye concentrations achieved an equilibrium state. It can be concluded that the batch system may function effectively for approximately 20-30 min at concentrations below 100 mg L-1 before requiring

Table 3. Isotherm parameters for the adsorption of AR18 and MB dyes using BW-AC adsorbent (Experimental conditions: adsorbent dosage = 1.5 g L^{-1} , contact time = 180 min, and natural pH of solutions)

la atha mar a ann an an	Investigated dye			
Isotherm parameter -	AR18	МВ		
Langmuir				
Q_{max} (mg g ⁻¹)	109.94	114.75		
K_L (L mg ⁻¹)	27.2	0.721		
R^2_{adj}	0.854	0.964		
SD	18.95	8.51		
RSS	3951.5	796.61		
AIC _c	83	62.167		
BIC	82	61.195		
Freundlich				
$K_f [mg g^{-1} (mg L^{-1})^{-1/nf}]$	85.49	43.175		
n _f	7.79	3.72		
R^2_{adj}	0.94	0.845		
SD	12.41	17.64		
RSS	1694.55	3423.28		
AIC _c	72	81.121		
BIC	71	80.149		
Liu				
Q _{max} (mg g ⁻¹)	741.35	115.83		
$K_g(L mg^{-1})$	1.044 × 10 ⁻⁵	0.693		
n_L	0.153	0.97		
R^2_{adj}	0.93	0.96		
SD	13	8.915		
RSS	1691.48	794.74		
AIC _c	76.3	66.47		
BIC	73.55	63.73		

regeneration (Figure 2 (A-D)).

To gain a deeper understanding of the impact of mass transfer resistance on the adsorption process, the intraparticle diffusion model was used. The plots of the amount of AR18 and MB adsorbed (q.) against the square root of time (t^{0.5}) exhibited a distinctly two-linear behavior for an initial dye concentration of 50 mg L⁻¹. In contrast, at a dye concentration of 100 mg L-1, a three-segment behavior was observed. Figure 2 (E-H) indicates that the adsorption process involves multiple rate-controlling steps, with each linear segment of the plot corresponding to a specific phase of the adsorption process (63,64). The initial linear segment, which represents the fastest adsorption stage, is associated with external surface adsorption, driven by the movement of dye molecules from the bulk solution to the external surface of the BW-AC adsorbent. The subsequent linear segment represents a delayed process attributed to intraparticle diffusion, involving the migration of dye molecules from the external surface into the internal pores of the BW-AC adsorbent. The third linear section, observed

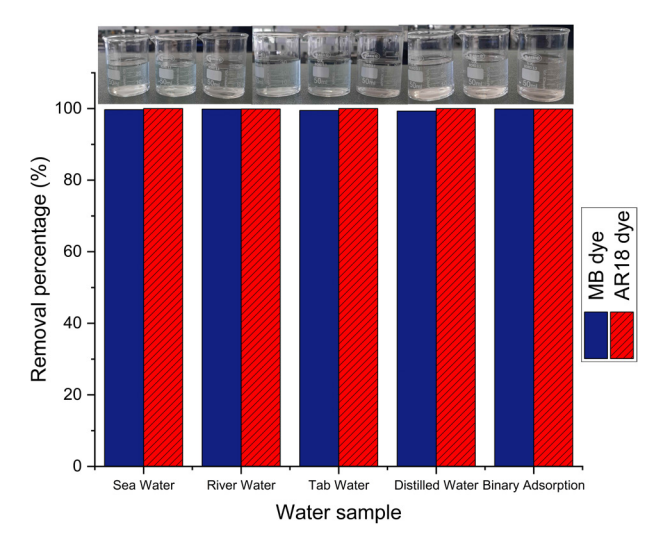


Figure 5. Adsorption of dyes from real water samples. Experimental conditions: natural pH; room temperature; contact time=180 min, BW-AC dosage=1.5 g L^{-1} , and initial dye concentration=100 mg L^{-1})

after reaching equilibrium, describes the diffusion of dye molecules through smaller pores within the BW-AC adsorbent. This phase highlights the continued movement of dye molecules as they navigate through the finer pore structures, contributing to the overall adsorption process. This multi-linearity behavior suggests that both external mass transfer and intraparticle diffusion mechanisms influenced the overall adsorption process (65,66).

Effect of adsorbent dosage

Adsorbent dosage is a critical factor in the adsorption process, as it directly influences adsorption capacity by determining the available surface area and active sites. Increasing the dosage enhances the adsorption rate by providing more surface area and active sites for dye molecules (63,66). Conversely, as the adsorbent dosage increased, the adsorption capacity (q_a) for both dyes decreased, reducing from 149.7 to 40 mg g-1 for AR18 and from 143 to 39.86 mg g⁻¹ for MB. This inverse relationship can be attributed to two main reasons: first, at a constant dye concentration, an increase in the adsorbent dosage results in the unsaturation of adsorption sites. Second, at higher adsorbent dosages, particle aggregation occurs, which diminishes the effective adsorption capacity and increases the diffusional path length (67). As shown in Figure 3, beyond a BW-AC dosage of 1.5 g L⁻¹, the removal efficiency did not significantly change. Therefore, this value was chosen as the optimal adsorbent dosage for subsequent experiments.

Effect of initial dye concentration and adsorption isotherms

Based on the investigated dye concentrations (5-250 mg L^{-1}), it can be concluded that the adsorbent dosage of 1.5 g L^{-1} effectively removes both dyes at concentrations up to 175 mg L^{-1} , establishing this as the optimal concentration

range for practical applications. As illustrated in Figure 4, the removal efficiency slightly decreased with increasing initial dye concentration, with a more obvious decline at higher concentrations. This behavior is attributed to the availability of sufficient adsorption sites at lower concentrations, enabling complete dye removal. At higher concentrations, however, the active sites on the adsorbent become saturated, leading to equilibrium and reduced adsorption efficiency (68).

Despite the decrease in removal efficiency, the adsorption capacity (q_e) of BW-AC increased significantly at higher initial dye concentrations. For AR18, q_e increased from 3.33 to 136 mg g⁻¹, while for MB, it increased from 3.22 to 116.5 mg g⁻¹. This trend is driven by the enhanced concentration gradient at higher dye concentrations, which provides a stronger driving force for mass transfer and promotes greater dye uptake (69).

Adsorption isotherms are valuable tools for describing the distribution of adsorbate molecules between the liquid and solid phases when the system reaches an equilibrium state. Isotherm models provide insights into the interactions between the adsorbent and adsorbate, helping to understand the mechanisms of adsorption and the efficiency of the adsorbent material (55,64). In the present study, nonlinear forms of the Langmuir, Freundlich, and Liu isotherm models were employed to investigate the adsorption isotherms.

The statistical parameters related to the fitted models are presented in Table 3. The correlation capability of the models, assessed using the AIC, and BIC, is ranked as follows: Freundlich, Liu, and Langmuir for AR18 dye; while for MB dye, the ranking is Langmuir, Liu, and Freundlich. The AIC values for the Langmuir and Freundlich models for AR18 dye were 83 and 72, respectively, indicating that the Freundlich model is 245.53 times more likely to be the best-fitted model compared to the Langmuir model. The BIC values for these models were 82 and 71, respectively. A BIC difference greater than 10 provides a decisive conclusion that the Freundlich model is indeed a better fit than the Langmuir model. For the comparison between the Freundlich and Liu models, the AIC values were 72 and 76.3, respectively, confirming that the Freundlich model is 8.63 times more likely to be the correct and best fit compared to the Liu model. The corresponding BIC values were 71 and 73.55, supporting the validity of the Freundlich model.

For MB dye, the AIC_c values were 62.167, 81.121, and 66.47 for the Langmuir, Freundlich, and Liu models, respectively. The Langmuir model for MB has the lowest AIC_c value, indicating a higher probability of being correct. Specifically, this model is 13055.1 times more likely to be correct compared to the Freundlich model and 8.6 times more likely than the Liu model. The BIC values for these models were 61.195, 80.149, and 63.73, respectively, which confirms a very strong support for

the Langmuir model compared to the Freundlich model and a positive support compared to the Liu model. For MB dye, the maximum adsorption capacity predicted by the Langmuir model was 114.75 mg g⁻¹, which aligns well with the experimental data, indicating the reliability of the model in predicting adsorption behavior.

Additionally, the higher R^2_{adj} and lower SD values for the Freundlich model suggest that it is the most suitable choice for fitting the isotherm data for the adsorption of AR18 onto BW-AC. In contrast, the Langmuir model demonstrated the highest R^2_{adj} and the lowest SD values for MB dye, indicating its superior accuracy compared to the other models for this system.

Unary and binary adsorption of dyes from real water samples

Figure 5 illustrates the adsorption performance of BW-AC in unary and binary systems across different water samples. The results indicate that the adsorbent exhibits a strong affinity for both dyes, with minimal interference from naturally occurring water constituents. The similar removal percentages observed for distilled water, seawater, well water, and tap water suggest that the adsorption process is not significantly affected by the ionic strength or composition of the water matrix. Furthermore, the binary adsorption experiments revealed no substantial competitive effects between AR18 and MB, as their removal percentages remained consistently high when adsorbed simultaneously. This demonstrates that the applied adsorbent dosage provides sufficient active sites to effectively adsorb both dyes without a notable decline in efficiency. These findings are particularly relevant for practical applications, highlighting the potential of BW-AC to treat dye-contaminated water across diverse environments, including industrial wastewater and natural water bodies.

Conclusion

In this study, BW-AC was prepared and evaluated for its effectiveness in adsorbing two commonly used dyes: AR18 and MB. Nearly complete dye removal was achieved with an adsorbent dosage $\geq 1.5~{\rm g\,L^{-1}}$. Bayesian analysis identified the general order kinetic model as the most suitable, with rapid adsorption half-lives (t_{1/2}: 0.00123–1.77 min for AR18; 0.18–0.28 min for MB) and equilibrium times (t_{0.95}: 0.72–143.32 min for AR18; 12–72.32 min for MB). Isotherm studies favored the Freundlich model for AR18 and the Langmuir model for MB.

Overall, BW-AC demonstrated high adsorption efficiency across various water matrices, confirming its potential as a low-cost, sustainable, and environmentally friendly adsorbent for the removal of dyes from contaminated effluents.

Acknowledgments

This research was approved and supported by the Cellular

and Molecular Biology Research Center, Health Research Institute, Babol University of Medical Sciences (IRCT code: IR.MUBABOL.HRI.REC.1403.177). The authors sincerely appreciate the Vice-Chancellor for Research and Technology of Babol University of Medical Sciences for their financial support. Additionally, the authors would like to thank the School of Public Health for providing the essential facilities needed to conduct this study.

Authors' contributions

Conceptualization: Hosseinali Asgharnia, Zeynab Gerinasab, Fatemeh Aligholizadeh, Hajar Tabarinia, Mohammad Shirmardi.

Data curation: Mahdieh Haddadi, Zeynab Gerinasab, Fatemeh Aligholizadeh, Hajar Tabarinia, Mohammad Shirmardi.

Formal Analysis: Mahdieh Haddadi, Mehdi Vosoughi, Mohammad Shirmardi.

Funding acquisition: Mohammad Shirmardi.

Investigation: Hosseinali Asgharnia, Mahdieh Haddadi, Zeynab Gerinasab, Fatemeh Aligholizadeh, Hajar Tabarinia, Mohammad Shirmardi.

Methodology: Hosseinali Asgharnia, Zeynab Gerinasab, Fatemeh Aligholizadeh, Mehdi Vosoughi, Hajar Tabarinia, Mohammad Shirmardi.

Project administration: Mohammad Shirmardi.

Resources: Hosseinali Asgharnia, Mehdi Vosoughi, Mohammad Shirmardi.

Software: Mahdieh Haddadi, Mohammad Shirmardi.

Supervision: Hosseinali Asgharnia, Mohammad Shirmardi.

Validation: Mahdieh Haddadi, Mehdi Vosoughi, Mohammad Shirmardi.

Visualization: Mahdieh Haddadi, Mehdi Vosoughi, Mohammad Shirmardi.

Writing-original draft: Hosseinali Asgharnia, Mahdieh Haddadi, Mehdi Vosoughi, Mohammad Shirmardi.

Writing-review & editing: Hosseinali Asgharnia, Mahdieh Haddadi, Mehdi Vosoughi, Mohammad Shirmardi.

Competing interests

The authors declare there are no conflicts of interest in the publication of this article.

Ethical issues

The authors certify that all data collected during the study are accurately represented in the manuscript, and no data from this study has been or will be published separately elsewhere (IRCT code: IR.MUBABOL.HRI. REC.1403.177).

Funding

This study received approval and support from the Cellular and Molecular Biology Research Center at the Health Research Institute, Babol University of Medical Sciences (IRCT code: IR.MUBABOL.HRI.REC.1403.177).

References

- de Almeida AP, Macrae A, Ribeiro BD, do Nascimento RP. Decolorization and detoxification of different azo dyes by Phanerochaete chrysosporium ME-446 under submerged fermentation. Braz J Microbiol. 2021;52(2):727-38. doi: 10.1007/s42770-021-00458-7.
- Rahimi S, Mohammadi F, Ghodsi S, Mohammadi M, Karimi H. Activation of persulfate by TiO2-Fe3O4 nanocomposite for reactive red 198 degradation along with modeling and optimization approach. Environ Health Eng Manag. 2023;10(2):165-77. doi: 10.34172/ehem.2023.19.
- Aragaw TA, Bogale FM. Biomass-based adsorbents for removal of dyes from wastewater: a review. Front Environ Sci. 2021;9:764958. doi: 10.3389/fenvs.2021.764958.
- Katheresan V, Kansedo J, Lau SY. Efficiency of various recent wastewater dye removal methods: a review. J Environ Chem Eng. 2018;6(4):4676-97. doi: 10.1016/j. jece.2018.06.060.
- Zafar S, Bukhari DA, Rehman A. Azo dyes degradation by microorganisms - an efficient and sustainable approach. Saudi J Biol Sci. 2022;29(12):103437. doi: 10.1016/j. sjbs.2022.103437.
- Dutta S, Adhikary S, Bhattacharya S, Roy D, Chatterjee S, Chakraborty A, et al. Contamination of textile dyes in aquatic environment: adverse impacts on aquatic ecosystem and human health, and its management using bioremediation. J Environ Manage. 2024;353:120103. doi: 10.1016/j.jenvman.2024.120103.
- Elsherif KM, Alkherraz AM, Edwards H, Mutawia BY. Congo red dye adsorption on dry green pea husk: effects of process parameters and modeling approaches. Environ Health Eng Manag. 2024;11(3):273-84. doi: 10.34172/ ehem.2024.27.
- 8. Nasrollahi P, Mirzaee SA, Gholami Z, Mansouri M, Noorimotlagh Z. Survey of catalytic performance of TiO2 via coupling with ZSM-5 zeolite under UV light for activation of peroxymonosulfate applied towards orange II (OII) degradation. Environ Health Eng Manag. 2023;10(4):419-28. doi: 10.34172/ehem.2023.45.
- Zare MR, Mengelizadeh N, Aghdavodian G, Zare F, Ansari Z, Hashemi F, et al. Adsorption of acid red 18 from aqueous solutions by GO-COFe2O4: adsorption kinetic and isotherms, adsorption mechanism and adsorbent regeneration. Desalin Water Treat. 2024;317:100219. doi: 10.1016/j.dwt.2024.100219.
- Bień T, Kołodyńska D, Franus W. Functionalization of zeolite NaP1 for simultaneous acid red 18 and Cu(II) removal. Materials (Basel). 2021;14(24):7817. doi: 10.3390/ ma14247817.
- 11. Baloo L, Isa MH, Sapari NB, Jagaba AH, Wei LJ, Yavari S, et al. Adsorptive removal of methylene blue and acid orange 10 dyes from aqueous solutions using oil palm wastesderived activated carbons. Alex Eng J. 2021;60(6):5611-29. doi: 10.1016/j.aej.2021.04.044.
- 12. Al-Ghouti MA, Al-Absi RS. Mechanistic understanding of the adsorption and thermodynamic aspects of cationic methylene blue dye onto cellulosic olive stones biomass from wastewater. Sci Rep. 2020;10(1):15928. doi: 10.1038/s41598-020-72996-3.
- 13. Kouhi K, Amouei A, Asgharnia H, Vosoughi M, Fallah SH,

- Shirmardi M. Application of oak charcoal-based activated carbon for the removal of methylene blue dye from aqueous solutions: kinetics, equilibrium, and reusability studies. Water Pract Technol. 2023;18(12):3255-70. doi: 10.2166/wpt.2023.203.
- 14. Peydayesh M, Rahbar-Kelishami A. Adsorption of methylene blue onto *Platanus orientalis* leaf powder: Kinetic, equilibrium and thermodynamic studies. J Ind Eng Chem. 2015;21:1014-9. doi: 10.1016/j.jiec.2014.05.010.
- 15. Lu F, Dong A, Ding G, Xu K, Li J, You L. Magnetic porous polymer composite for high performance adsorption of acid red 18 based on melamine resin and chitosan. J Mol Liq. 2019;294:111515. doi: 10.1016/j.molliq.2019.111515.
- Bazrafshan E, Kord Mostafapour F. Evaluation of color removal of methylene blue from aqueous solutions using plant stem ash of persica. J North Khorasan Univ Med Sci. 2013;4(4):523-32. doi: 10.29252/jnkums.4.4.523. [Persian].
- Gholami-Borujeni F, Naddafi K, Nejatzade-Barandozi F. Application of catalytic ozonation in treatment of dye from aquatic solutions. Desalin Water Treat. 2013;51(34-36):6545-51. doi: 10.1080/19443994.2013.769491.
- 18. Askari R, Mohammadi F, Moharrami A, Afshin S, Rashtbari Y, Vosoughi M, et al. Synthesis of activated carbon from cherry tree waste and its application in removing cationic red 14 dye from aqueous environments. Appl Water Sci. 2023;13(4):90. doi: 10.1007/s13201-023-01899-1.
- 19. Ashournezhad H, Asgharnia H, Ahmad Nateghi S, Ebrahimi A, Heydari M, Akbari A, et al. Comparison of the efficiency of synthesized magnesium oxide (MgO) nanoparticles and powdered activated carbon (PAC) for the adsorption of acid red 18 dye from aqueous solutions. J Mazandaran Univ Med Sci. 2023;33(1):258-73. [Persian].
- 20. Afshin S, Rashtbari Y, Shirmardi M, Vosoughi M, Hamzehzadeh A. Adsorption of basic violet 16 dye from aqueous solution onto mucilaginous seeds of *Salvia sclarea*: kinetics and isotherms studies. Desalin Water Treat. 2019;161:365-75. doi: 10.5004/dwt.2019.24265.
- 21. Dutta S, Gupta B, Srivastava SK, Gupta AK. Recent advances on the removal of dyes from wastewater using various adsorbents: a critical review. Mater Adv. 2021;2(14):4497-531. doi: 10.1039/d1ma00354b.
- Mousavi SA, Shahbazi D, Mahmoudi A, Darvishi P. Methylene blue removal using prepared activated carbon from grape wood wastes: adsorption process analysis and modeling. Water Qual Res J. 2022;57(1):1-9. doi: 10.2166/ wqrj.2021.015.
- Shirmardi M, Mahvi AH, Mesdaghinia A, Nasseri S, Nabizadeh R. Adsorption of acid red 18 dye from aqueous solution using single-wall carbon nanotubes: kinetic and equilibrium. Desalin Water Treat. 2013;51(34-36):6507-16. doi: 10.1080/19443994.2013.793915.
- 24. Rajoria S, Vashishtha M, Sangal VK. Treatment of electroplating industry wastewater: a review on the various techniques. Environ Sci Pollut Res. 2022;29(48):72196-246. doi: 10.1007/s11356-022-18643-y.
- 25. Adibzadeh A, Khodabakhshi MR, Maleki A. Preparation of novel and recyclable chitosan-alumina nanocomposite as superabsorbent to remove diazinon and tetracycline contaminants from aqueous solution. Heliyon. 2024;10(1):e23139. doi: 10.1016/j.heliyon.2023.e23139.
- 26. Shirmardi M, Mahvi AH, Hashemzadeh B, Naeimabadi A, Hassani G, Vosoughi Niri M. The adsorption of malachite green (MG) as a cationic dye onto functionalized

- multi walled carbon nanotubes. Korean J Chem Eng. 2013;30(8):1603-8. doi: 10.1007/s11814-013-0080-1.
- Roohbakhsh Bidaei M, Azadfallah M, Yarahmadi R, Goleij N. Production of activated carbon from decayed wood: surface modification using high-frequency DBD plasma for enhanced rhodamine B dye adsorption--a kinetic and equilibrium study. BioResources. 2024;19(4):9510-30. doi: 10.15376/biores.19.4.9510-9530.
- 28. Alvan Sabet Company. 2025. Available from: https://www.alvansabet.ir/product/ariacid-brill-scarlet-3r/.
- 29. Shahryari Z, Soltani Goharrizi A, Azadi M. Experimental study of methylene blue adsorption from aqueous solutions onto carbon nano tubes. Int J Water Res Environ Eng. 2010;2(2):16-28.
- Tan KL, Hameed BH. Insight into the adsorption kinetics models for the removal of contaminants from aqueous solutions. J Taiwan Inst Chem Eng. 2017;74:25-48. doi: 10.1016/j.jtice.2017.01.024.
- 31. Liu Y, Shen L. A general rate law equation for biosorption. Biochem Eng J. 2008;38(3):390-4. doi: 10.1016/j. bej.2007.08.003.
- 32. Liu Y, Liu YJ. Biosorption isotherms, kinetics and thermodynamics. Sep Purif Technol. 2008;61(3):229-42. doi: 10.1016/j.seppur.2007.10.002.
- 33. Ho YS. Review of second-order models for adsorption systems. J Hazard Mater. 2006;136(3):681-9. doi: 10.1016/j. jhazmat.2005.12.043.
- 34. Weber WJ Jr, Morris JC. Kinetics of adsorption on carbon from solution. J Sanit Eng Div. 1963;89(2):31-59. doi: 10.1061/jsedai.0000430.
- 35. Cardoso NF, Lima EC, Pinto IS, Amavisca CV, Royer B, Pinto RB, et al. Application of cupuassu shell as biosorbent for the removal of textile dyes from aqueous solution. J Environ Manage. 2011;92(4):1237-47. doi: 10.1016/j.jenvman.2010.12.010.
- 36. Sukla Baidya K, Kumar U. Adsorption of brilliant green dye from aqueous solution onto chemically modified areca nut husk. S Afr J Chem Eng. 2021;35:33-43. doi: 10.1016/j. sajce.2020.11.001.
- 37. Langmuir I. The adsorption of gases on plane surfaces of glass, mica and platinum. J Am Chem Soc. 1918;40(9):1361-403. doi: 10.1021/ja02242a004.
- 38. Freundlich H. Adsorption in solution. Phys Chem Soc. 1906;40:1361-8.
- Liu Y, Xu H, Yang SF, Tay JH. A general model for biosorption of Cd2+, Cu2+ and Zn2+ by aerobic granules.
 J Biotechnol. 2003;102(3):233-9. doi: 10.1016/s0168-1656(03)00030-0.
- 40. Trivedi S, Belgamwar V, Wadher K, Umekar M. Development and validation of a UV spectrophotometric method for the estimation of the synthesized lentinan–Congo red complex. J Appl Spectrosc. 2022;89(2):344-9. doi: 10.1007/s10812-022-01364-y.
- Ostaszewski P, Długosz O, Banach M. Analysis of measuring methods of the concentration of methylene blue in the sorption process in fixed-bed column. Int J Environ Sci Technol. 2022;19(1):1-8. doi: 10.1007/s13762-021-03156-x.
- 42. Akinremi CA, Adeogun AI, Poupin M, Huddersman K. Chitosan-terephthalic acid-magnetic composite beads for effective removal of the acid blue dye from aqueous solutions: kinetics, isotherm, and statistical modeling. ACS Omega. 2021;6(45):30499-514. doi: 10.1021/

- acsomega.1c03964.
- 43. Spiess AN, Neumeyer N. An evaluation of R2 as an inadequate measure for nonlinear models in pharmacological and biochemical research: a Monte Carlo approach. BMC Pharmacol. 2010;10:6. doi: 10.1186/1471-2210-10-6.
- 44. Vareda JP. On validity, physical meaning, mechanism insights and regression of adsorption kinetic models. J Mol Liq. 2023;376:121416. doi: 10.1016/j.molliq.2023.121416.
- 45. Akaike H. A new look at the statistical model identification. IEEE Trans Automat Contr. 2003;19(6):716-23. doi: 10.1109/tac.1974.1100705.
- 46. Sugiura N. Further analysis of the data by Akaike's information criterion and the finite corrections: further analysis of the data by Akaike's. Commun Stat Theory Methods. 1978;7(1):13-26. doi: 10.1080/03610927808827599.
- 47. Sakamoto Y, Ishiguro M, Kitagawa G. Akaike Information Criterion Statistics. Dordrecht, The Netherlands: Springer Netherlands; 1986. p. 290.
- 48. Burnham KP, Anderson DR. Multimodel inference: understanding AIC and BIC in model selection. Sociol Methods Res. 2004;33(2):261-304. doi: 10.1177/0049124104268644.
- 49. Emiliano PC, Vivanco MJ, de Menezes FS. Information criteria: how do they behave in different models? Comput Stat Data Anal. 2014;69:141-53. doi: 10.1016/j. csda.2013.07.032.
- 50. Dan-Iya BI, Yahuza S, Sabo IA, Faggo AA, Khayat ME. Isothermal modelling of the adsorption of malachite green onto rice husks. Bull Environ Sci Sustain Manage. 2023;7(1):58-65. doi: 10.54987/bessm.v7i1.904.
- 51. Sabo IA, Yahuza S, Dan-Iya BI, Abubakar A. Kinetic analysis of the adsorption of malachite green onto graphene oxide sheets integrated with gold nanoparticles. J Biochem Microbiol Biotechnol. 2021;9(2):48-52. doi: 10.54987/jobimb.v9i2.618.
- 52. Lima ÉC, Pinto D, Schadeck Netto M, Dos Reis GS, Silva LF, Dotto GL. Biosorption of neodymium (Nd) from aqueous solutions using *Spirulina platensis* sp. strains. Polymers (Basel). 2022;14(21):4585. doi: 10.3390/polym14214585.
- 53. Franco DS, Georgin J, Ramos CG, Netto MS, Lobo B, Jimenez G, et al. Production of adsorbent for removal of propranolol hydrochloride: use of residues from *Bactris guineensis* fruit palm with economically exploitable potential from the Colombian Caribbean. J Mol Liq. 2023;380:121677. doi: 10.1016/j.molliq.2023.121677.
- 54. Lorah J, Womack A. Value of sample size for computation of the Bayesian information criterion (BIC) in multilevel modeling. Behav Res Methods. 2019;51(1):440-50. doi: 10.3758/s13428-018-1188-3.
- 55. Ibrahim HA, Abdel Moamen OA, Monem NA, Ismail IM. Assessment of kinetic and isotherm models for competitive sorption of Cs+and Sr2+from binary metal solution onto nanosized zeolite. Chem Eng Commun. 2018;205(9):1274-87. doi: 10.1080/00986445.2018.1446004.
- 56. Nayak AK, Pal A. Development and validation of an adsorption kinetic model at solid-liquid interface

- using normalized Gudermannian function. J Mol Liq. 2019;276:67-77. doi: 10.1016/j.molliq.2018.11.089.
- Anderson DR, Burnham KP. Model Selection and Multi-Model Inference. New York, NY: Springer; 2004. p. 488.
- 58. Nizam NU, Hanafiah MM, Mahmoudi E, Mohammad AW. Synthesis of highly fluorescent carbon quantum dots from rubber seed shells for the adsorption and photocatalytic degradation of dyes. Sci Rep. 2023;13(1):12777. doi: 10.1038/s41598-023-40069-w.
- 59. Rahman MS. Adsorption of methyl blue onto activated carbon derived from red oak (*Quercus rubra*) acorns: a 26 factorial design and analysis. Water Air Soil Pollut. 2020;232(1):1. doi: 10.1007/s11270-020-04943-x.
- 60. Namasivayam C, Kavitha D. Removal of Congo red from water by adsorption onto activated carbon prepared from coir pith, an agricultural solid waste. Dyes Pigm. 2002;54(1):47-58. doi: 10.1016/s0143-7208(02)00025-6.
- 61. Singh NB, Agrawal S, Rachna K. Methylene blue dye removal from water by nickel ferrite polyaniline nanocomposite. J Sci Ind Res. 2019;78(2):118-21.
- 62. Tong DS, Wu CW, Adebajo MO, Jin GC, Yu WH, Ji SF, et al. Adsorption of methylene blue from aqueous solution onto porous cellulose-derived carbon/montmorillonite nanocomposites. Appl Clay Sci. 2018;161:256-64. doi: 10.1016/j.clay.2018.02.017.
- 63. Shirmardi M, Alavi N, Lima EC, Takdastan A, Mahvi AH, Babaei AA. Removal of atrazine as an organic micropollutant from aqueous solutions: a comparative study. Process Saf Environ Prot. 2016;103(Pt A):23-35. doi: 10.1016/j.psep.2016.06.014.
- 64. Martins AC, Pezoti O, Cazetta AL, Bedin KC, Yamazaki DA, Bandoch GF, et al. Removal of tetracycline by NaOH-activated carbon produced from macadamia nut shells: kinetic and equilibrium studies. Chem Eng J. 2015;260:291-9. doi: 10.1016/j.cej.2014.09.017.
- 65. Singh S, Yadawa Y, Ranjan A. Enhanced adsorption of methylene blue by mixed-phase bismuth ferrite prepared by non-aqueous sol-gel route. J Environ Chem Eng. 2023;11(1):109229. doi: 10.1016/j.jece.2022.109229.
- 66. dos Reis GS, Bergna D, Grimm A, Lima EC, Hu T, Naushad M, et al. Preparation of highly porous nitrogen-doped biochar derived from birch tree wastes with superior dye removal performance. Colloids Surf A Physicochem Eng Asp. 2023;669:131493. doi: 10.1016/j.colsurfa.2023.131493.
- 67. Masoumi H, Ghaemi A, Ghanadzadeh Gilani H. Surveying the elimination of hazardous heavy metal from the multicomponent systems using various sorbents: a review. J Environ Health Sci Eng. 2022;20(2):1047-87. doi: 10.1007/s40201-022-00832-z.
- 68. Thakur V, Sharma P, Awasthi A, Guleria A, Singh K. Utility of acrylic acid grafted lignocellulosic waste sugarcane bagasse for the comparative study of cationic and anionic dyes adsorption applications. Environ Nanotechnol Monit Manag. 2023;20:100824. doi: 10.1016/j.enmm.2023.100824.
- 69. Bharathi KS, Ramesh ST. Removal of dyes using agricultural waste as low-cost adsorbents: a review. Appl Water Sci. 2013;3(4):773-90. doi: 10.1007/s13201-013-0117-y.